Pressure Effects on the Joint Elastic-electrical Properties of Shaly Sandstones based on Clay Distribution.

Najeeb Aladwani [a,b] , Laurence J. North[b,] & Angus I. Best[b] ,
[a]University of Southampton, [b]National Oceanography Centre
Contact email: nska1g13@soton.ac.uk

Introduction

The advent of marine controlled source electromagnet (CSEM) surveying techniques for oil and gas exploration in the early 2000s, used to supplement co-located seismic surveys (MacGregor et al. 1998), has led to increased interest in joint elastic and electrical properties of reservoir and overburden rocks and sediments (Han et al. 2016). A better understanding of these inter-relationships is needed to improve quantitative interpretation of geophysical data for reservoir exploration, characterization and monitoring (Hoversten et al. 2006; Harris et al. 2009).

In this study, we further analyze the laboratory data of Han et al. (2011) in terms of pressure effects in shaly sandstone that have been classified into four groups according to clay distribution (see Aladwani et al, 2016). We were able to identify distinctly different influences of load-bearing and pore-filling clay minerals on velocity, attenuation and electrical resistivity, important features that should be included in the development of joint properties models.

Methods

We reproduced parameter cross-plots from Han et al. (2011) showing the pressure sensitivity of relations among elastic-electrical properties (ultrasonic P- & S-wave velocity Vp, Vs; ultrasonic P- & S-wave attenuation Qp^{-1}, Qs^{-1}; electrical resistivity ρ), but with the new clay distribution classification superimposed; Han et al. (2011) previously only indicated total clay content, not clay distribution. We followed the clay distribution classification technique of Sørensen et al. (2015), adapted to our particular dataset. It is based on core sample measurements of clay mineral volume percent, porosity, and brine (35 g/L) saturated P- & S-wave velocity, and comparison of the calculated dry frame P-wave modulus to that of a theoretical modified Hashin-Shtrikman bound; see methods and results reported for the same dataset at a single effective pressure in Aladwani et al. (2016). The four clay distribution classes were: clean sandstone (green symbols in Figure 1); partially pore-filling clay (pink); homogeneous pore-filling clay (red symbols); and load-bearing clay (black).

Example results

Figure 1 shows G2, the pressure sensitivity (in the range 8 – 60 MPa) of the relationship between resistivity ρ and P-wave attenuation 1000/Qp, plotted against 1000/Qp, and that of G3 (Vp -1000/Qp pressure sensitivity) against porosity. We can see that sandstones with load-bearing clay generally have the higher (i.e. more negative and larger magnitude) G2 pressure sensitivity than sandstones with pore-filling clay (although the latter group shows a wide scatter). Also, we see lower magnitude (less negative) G3 pressure sensitivity at porosities 10 – 13%, equivalent to the critical porosity when sand

grain pores are filled with clay, otherwise G3 is more sensitive (larger magnitude, more negative) for load-bearing clay than for pore-filling clay. This relates to the degree of heterogeneity of mineral grains in these shaly sandstones.

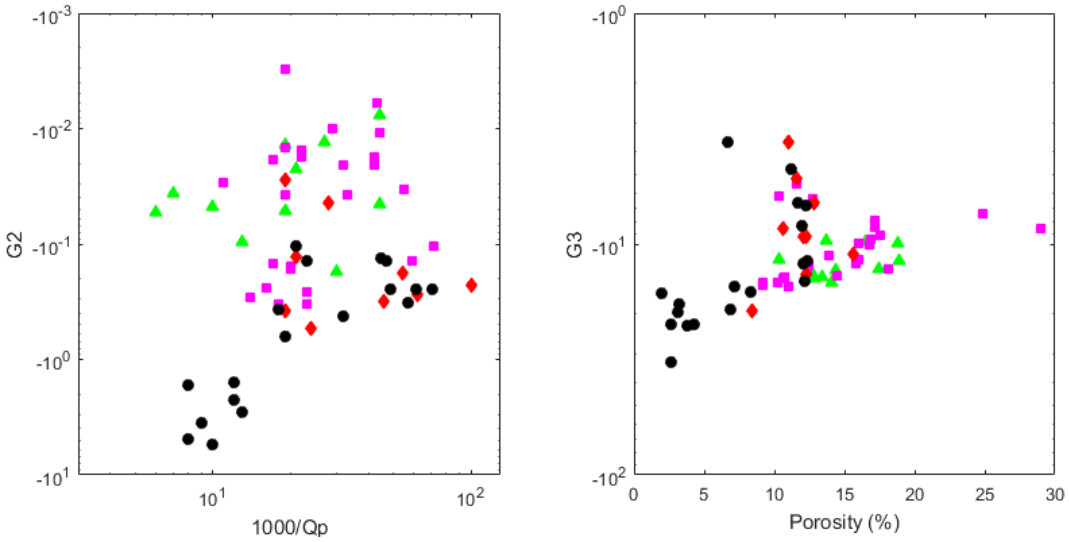

Figure 1: scatter diagrams showing (left) the relationship between G2 (resistivity - 1000/Qp pressure sensitivity) against 1000/Qp, and (right) G3 (Vp – 1000/Qp pressure sensitivity) versus porosity. Note log scale on y-axes. Colours represent the different clay classifications (see text).

Conclusions

Using a clay classification scheme based on ultrasonic velocity measurements, we were able to identify how load - bearing clay and partial pore-filling clay affect the pressure sensitivity of relationships among electrical resistivity, ultrasonic velocity and attenuation for differential pressures 8 – 60 MPa, as compared to petrophysical properties (e.g. porosity). The results are useful for developing and calibrating rock physics models for geopressure prediction.

References

Aladwani, N. et al., 2016. Clay Distribution Effects on the Joint Elastic-electrical Properties of Shaly Sandstones. In *78th EAGE Conference and Exhibition 2016*.

Han, T. et al., 2016. Are self-consistent models capable of jointly modeling elastic velocity and electrical conductivity of reservoir sandstones ? , 81(4), pp.363–368.

Han, T. et al., 2011. Pressure effects on the joint elastic-electrical properties of reservoir sandstones. *Geophysical Prospecting*, 59, pp.506–517.

Harris, P.E. et al., 2009. Joint interpretation of seismic and CSEM data using well log constraints: An example from the Luva Field. *first break*, 27(5).

Hoversten, G.M. et al., 2006. Direct reservoir parameter estimation using joint inversion of marine seismic AVA and CSEM data. *Geophysics*, 71(3), p.C1.

MacGregor, L.M., Constable, S. & Sinha, M.C., 1998. The RAMESSES experiment - III. Controlled-source electromagnetic sounding of the Reykjanes Ridge at 57 degrees 45 â€™ N. *Geophysical Journal International*, 135(3), pp.773–789.

Sørensen, M., Best, A.I. & Fabricius, I., 2015. Classification of sandstone by shale distribution and the effects on saturated elastic moduli. *3Iwrp.Org*, pp.1–4. Available at: http://3iwrp.org/submissions/abstracts/AB_MS20141211-RAD89CCB.pdf.